The Mathematical Model and Applications of Coded Structured Light System for Object Detecting

Xiaojun Jia[1]
[1]College of Mathematics and Information Engineering, Jiaxing University, Jiaxing, China
Email: xjjia@mail.zjxu.edu.cn

Guangxue Yue[1,2], Fang Mei[1]
[1]College of Mathematics and Information Engineering, Jiaxing University, Jiaxing, China
[2]College of computer & communication, Hunan University, Changsha,, China
Email: {guangxueyue, fangmei}@163.com

***Abstract*—According to the sensing principle of coded structured light, and the characteristics of broad complication and high parameters request, a new coded structured light mathematics model and measurement method is proposed, which can simply and quickly obtain depth information of targets. Model is simulated by computer. It can gain the offset and deformation of pattern images based on different model parameters. For the deformation of images, system parameters can be changed correspondingly. So, whole system can be fixed on using optimal system parameters. The experiment results reveal that the method of structured light model and simulation proposed are reasonable and effective, which have important theoretical value and practical signification.**

***Index Terms*—coded structure light, model, object detecting, reconstruction**

I. INTRODUCTION

Coded structured light sensing system [1-3] usually consists of a light source and a camera(CCD). The light source device projects a pattern or a set of patterns to scene, and through analyzing the pattern deformations that appear in grabbed images of every projection with CCD, 3D information of the object surface can be calculated based on the triangle principle and decoding algorithm.

In coded structured light sensing system, sensing precision and vision scope highly depend on several key parameters of system structure: distance between CCD and light source device, visual angle of CCD, visual angle of light source, distance between pattern and light source and distance between image plane and CCD. These parameters must be preprocessed, which is also an extremely tedious process. References [4-6] have given usual models of structured light sensing system and generic methods of gaining depth information. However, these methods whose derived relations are complex, and errors are high. This paper presents a new structured light mathematical model based on the luminous spot position both pattern and image plane to calculate goal depth information, which is simple and quick. In order to confirm system parameters, model simulation beforehand using the computer is processed. With system parameters changing, pattern image grabbed will displace and distort. According to the deformation of the image's situation, the optimum system parameters will be obtained, and the model can be finally finalized.

This work is partially supported by the Research Foundation of Science and Technology Bureau of Jiaxing (No:2008AY2014), and the Natural Science Foundation of Zhejiang Province of China under grant(No:Y1080901).

Xiaojun Jia is the corresponding author.

II. STRUCTURED LIGHT SYSTEM MODEL

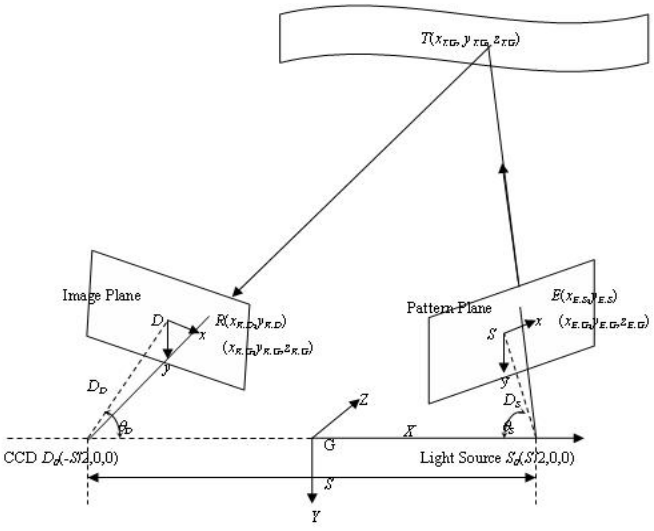

Figure 1. Structured light system's pinhole model

Ideal structured light sensing system model shown in Figure 1 includes spot light source $S_0(S/2,0,0)$, CCD $D_0(-S/2,0,0)$, pattern plane S, image plane D. 3D world coordinates system is established whose coordinates'

origin is the center point of segment between light source and CCD optical center point. The *Z* axis plumps paper surface and it points to inner. The coordinates system conforms to the right-hand rule. Plane *S* expresses pattern image. Line through both plane *S* geometric center and light source S_0 is vertical to plane *S*, whose included angle to *X* axis is θ_S, and the distance is D_S. Plane *D* is object image plane. Line through both plane *D* geometric center and CCD optical center is vertical to plane *D*, whose included angle to *X* axis is θ_D, and the distance is D_D. *T* is goal point in 3D scene. Supposed that the intersection between spatial line TS_0 and plane *S* is *E*, and the intersection of spatial line TD_0 and plane *D* is *R*. According to the model, depth information of *T* can be calculated based on triangle principle.

The intersection between spatial lines TS_0 and TD_0 is 3D coordinates of *T*. In order to analyze the structured light system, supposed that the system satisfies pinhole model. Projecting Figure 1 to plane *XGZ*, and the projection is separated into two sub-images shown in Figure 2(a) and (b) for light source side and CCD side respectively. At the side of light source shown in Figure 2(a), SH_S is vertical to *x* axis, and H_S is the intersection. x' axis is parallel to *x* axis, and *S* is the intersection. *EHE* is vertical to x' axis, and H_E is the intersection. α_S is the included angle from TS_0 to x axis. At the side of CCD, shown in Figure 2(b), DH_D is vertical to x axis, and H_D is the intersection. x' axis is parallel to *x* axis, and *D* is the intersection. RH_R is vertical to x' axis, and H_R is the intersection. α_D is the included angle from TD_0 to *x* axis. Using the triangle geometry relations, a series of equations can be expressed as fellow.

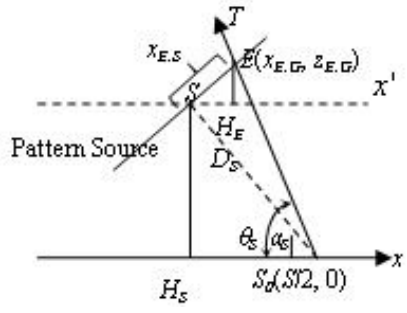

(a) Three-cornered relation of light source side

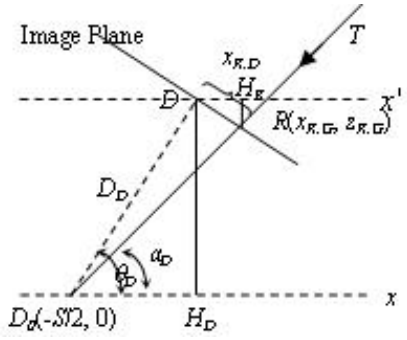

(b) Three-cornered relation of CCD side

Figure 2. Three-cornered relation of projection

A. Coordinate Transformation Relations

At the side of light source, we suppose that the coordinates of *E* are $(x_{E.S}, y_{E.S})$ in plane *S* coordinate system, and its coordinates in 3D coordinate system *G* are $(x_{E.G}, y_{E.G}, z_{E.G})$. According to Figure 1 and Figure 2(a), triangle SH_EE is similar to triangle $SHsS_0$, which can be expressed as:

$$\begin{cases} x_{E.G} = S/2 - D_S \times \cos\theta_S + x_{E.S} \times \sin\theta_S \\ y_{E.G} = y_{E.S} \\ z_{E.G} = D_S \times \sin\theta_S + x_{E.S} \times \cos\theta_S \end{cases} \quad (1)$$

Likewise, at the side of CCD, we can obtain planar point $R(x_{R.D}, y_{R.D})$ of spatial point $T(x_{R.G}, y_{R.G}, z_{R.G})$ in image. According to Figure 1 and Figure 2(b), triangle DRH_R is similar to triangle DD_0H_D. Comparing with (1), its equation is:

$$\begin{cases} x_{R.G} = -S/2 + D_D \times \cos\theta_D + x_{R.D} \times \sin\theta_D \\ y_{R.G} = y_{R.D} \\ z_{R.G} = D_D \times \sin\theta_D - x_{R.D} \times \cos\theta_D \end{cases} \quad (2)$$

B. Depth Information Calculation

We observe that coordinates of $R(x_{R.D}, y_{R.D})$ in image plane corresponds to *D* coordinate. Through decoding algorithm, and point $E(x_{E.S}, y_{E.S})$ in pattern corresponds to point *R*. According to the above, we may calculate spatial coordinates of target *T* as follows:

$$\begin{cases} \alpha_S = \theta_S + tg^{-1}(x_{E.S} / D_S) \\ \alpha_D = \theta_D - tg^{-1}(x_{R.D} / D_D) \end{cases} \quad (3)$$

And:

$$S = z_{T.G} \times ctg\alpha_S + z_{T.G} \times ctg\alpha_D \quad (4)$$

Combining (1) and (2), $z_{T.G}$ is expressed by the equation:

$$z_{T.G} = S \times \frac{\sin\alpha_S \times \sin\alpha_D}{\sin(\alpha_S + \alpha_D)} \quad (5)$$

And:

$$\begin{aligned} x_{T.G} &= S/2 - z_{T.G} \times ctg\alpha_S \\ &= S/2 \times \frac{\sin(\alpha_S - \alpha_D)}{\sin(\alpha_S + \alpha_D)} \end{aligned} \quad (6)$$

In addition, in the *YGD* plane, there is:

$$\frac{y_{E.S}}{y_{T.G}} = \frac{z_{E.G}}{z_{T.G}} = \frac{D_S \times \sin\theta_S + x_{E.S} \times \cos\theta_S}{S \times \frac{\sin\alpha_S \times \sin\alpha_D}{\sin(\alpha_S + \alpha_D)}} \quad (7)$$

So:

$$y_{T.G} = \frac{S \times (\sin\alpha_S \times \sin\alpha_D) \times y_{E.S}}{\sin(\alpha_D + \alpha_S) \times (D_S \times \sin\theta_S + x_{E.S} \times \cos\theta_S)} \quad (8)$$

Combining (5), (6) and (8), the spatial coordinates of *T* is:

$$\begin{cases} x_{T.G} = S/2 \times \dfrac{\sin(\alpha_S - \alpha_D)}{\sin(\alpha_S + \alpha_D)} \\ y_{T.G} = \dfrac{S \times (\sin\alpha_S \times \sin\alpha_D) \times y_{E.S}}{\sin(\alpha_D + \alpha_S) \times (D_S \times \sin\theta_S + x_{E.S} \times \cos\theta_S)} \\ z_{T.G} = S \times \dfrac{\sin\alpha_S \times \sin\alpha_D}{\sin(\alpha_S + \alpha_D)} \end{cases} \quad (9)$$

III. System Simulation Experiments

Before applying the structured light model to practical scene, it is necessary that the system optimal parameters should be decided to finalize the sensing system. We develop a set of software system to adjust model parameter based on Borland C++ Builder 6.0 and Intel OpenCV computer vision library.

At fist, we must choose experiment parameters and their expression methods. The distance of light source and CCD: S; The distance between light source and pattern: D_S , included angle: S_Degree ; The distance between CCD and image plane: D_D , included angle: D_Degree ;Depth information: Z.

In experiments, to clearly display displacement and distortion pattern in image, partial pattern is put into projecting. In fact, the experimental results have nothing to do with the projection pattern, even if the pattern consists of Chinese character or other small sub-image, the similar experimental results can be obtained. Projection pattern is shown in Figure 3, whose size is 121 ×121 pixels. The image plane size is 640×400 pixels. The unit of length is millimeter (mm), and the unit of angle is degree (°).

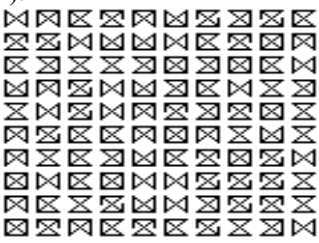

Figure 3. Projection pattern (Enlargement)

A. The Fist Simulation Experiment

S、 D_S 、 D_D 、 S_Degree and D_Degree are invariable, but Z changes gradually. We take 20 values separately to observe the change of image, such as 1000, 1200, 1400, 1800, 2000, 3000, and so on. Two experimental results are shown in Figure 4.

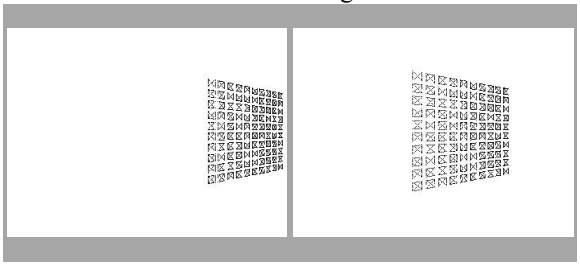

(a)The image at 1000mm (b)The image at 2000mm

Figure 4. Images under different Z values

With the Z changing from small to big, the image will gradually shift from right go left in the image plane, and it will grow big. At the same time, it does not maintain consistent with primitive image's position and size. If Z is big enough, the image will arrive at the boundary of image plane. Theoretically, the bigger the depth, the bigger symbols in the pattern will increase in the scene. Because of included angles of light source side and CCD side, images don't keep consistent result with primitive image's position and size even though depth Z changes big. Experimental result shows that even if the depth value is very big under determinate S、 D_S 、 D_D 、 S_Degree and D_Degree , the pattern image may also be observed in image plane. Certainly, once Z is big enough, such as 50000mm, because of counting error, the image will become fuzzy, and cross the border of image plane.

B. The Second Simulation Experiment

S、 D_S 、 D_D and Z are invariable, but D_Degree is variable. To simplify the experiment parameters, S_Degree and D_Degree are assigned same value. In fact, they can be different value. The angles assign 45, 60, 65, 75, 80, 89, 89.9 degrees and so on. Two experiment results are shown in Figure 5.

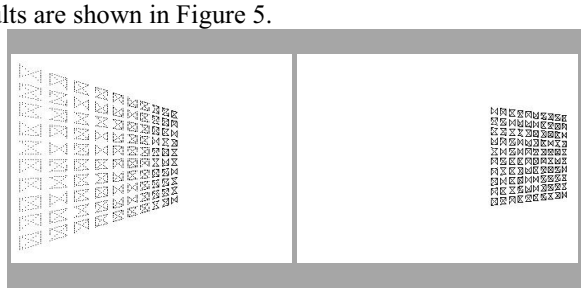

(a)The image at 60 degree (b)The image at 80 degree

Figure 5. Images with S_Degree and D_Degree changing

Different angles have a crucial influence to image size. When the angle is small, the change of depth of scene changes is small. When the angle gradually approaches to 90 degrees, image likely reaches the primitive pattern's size. Although we may theoretically obtain the image whose size is same with original pattern, if pattern is too big to observe whole image. Because there is certain distance between light source and CCD, which names invisible region, therefore, we must adopt the suitable angles to avoid this situation occurring.

C. The Third Simulation Experiment

S、 S_Degree 、 D_Degree and Z are invariable, but D_S and D_D can change. And D_S and D_D have the same value. In the experiment, 20 different values are chosen to use, such as 50mm、80mm、100mm and so on, and 20

different images are obtained. There are two images shown Figure 6.

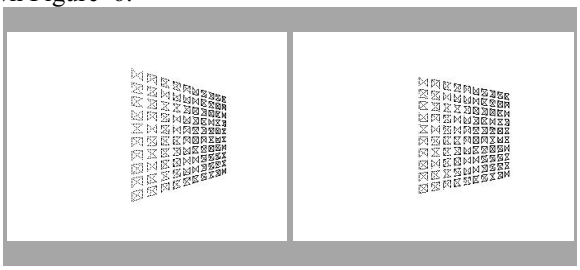

(a) The image at 50mm (b) The image at 80mm

Figure 6. Images with D_S and D_D changing

D_S and D_D have the crucial role to influence on image size. The smaller its value is, the more serious the deformation of the image is. The bigger its value is, the closer approaches to the primitive pattern. However, the scene depth and area inevitably influence pattern's size and request the bigger image plane, which contravenes the actual request. Suitable D_S and D_D may satisfy not only the image request but also making the pattern small. It can achieve measurement request.

D. The Fourth Simulation Experiment

D_S 、 D_D 、 S_Degree 、 D_Degree and Z are invariable, but S changes. 30 different values are chosen to use, such as 400mm, 800mm, 1400mm, 1800mm and so on. Two images are shown in Figure 7.

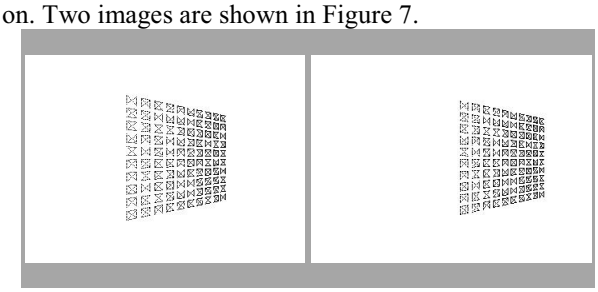

(a) The image at 800mm (b) The image at 1200mm

Figure 7. Images with *S* changing

Different *S* has tremendously influences to the image position and distortion. The smaller *S* value is, the fiercer deformation of the image is. The bigger S value is, the closer approaches to primitive pattern. At the same time, the image will be reformatting seriously. Theoretically, the structured light sensing principle is based on trigonometry. When one side of triangle changes, the distance form its opposite angle apex to the side will badly change. In practical application, we usually need to consider the size and portability of model Therefore. So the *S* is not too big.

E. Simulation Experiment Conclusions

Comparing with and analyzing different experiment results, we may summarize for the system parameters as follows:

- D_S and D_D have the key roles. Even if they are small, the image will have serious distortion.
- S_Degree and D_Degree have crucial influences to sense depth information, and because of them, invisible region may appear.
- *S* has a key role influences to image deformation. Thinking about the serviceability of installment, it is necessary for us to change suitable S.

Figure 8 shows the established experiment platform which based on the following group of parameters: S=900mm, D_S and D_D =65mm, S_Degree and D_Degree =75.

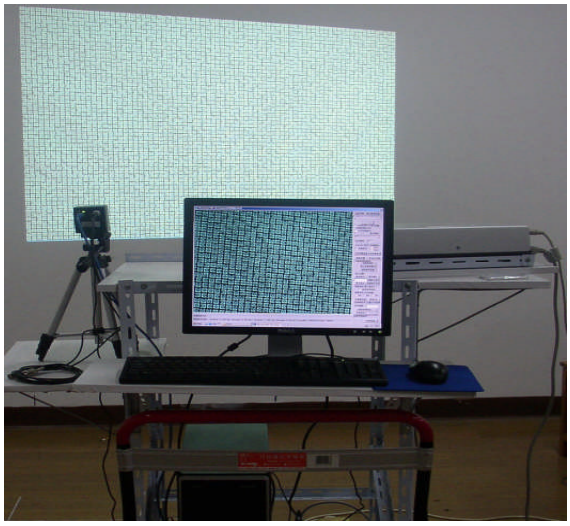

Figure 8. Structured light sensing platform

IV. MODEL APPLICATIONS

Using the established experiment platform to detect the objects in scene, we propose the code pattern, the codification and the three dimensional reconstruction.

A. Code Pattern

M array pattern is one of the most suitable pattern to use in the dynamic scene, which complete encoding using the space encoding on the two axle, and the sub-pattern' size being n×m. The sub-pattern owns a globe unique code in whole pattern to make it suitable for moving objects sensing at one-shot. Sub-patterns are be recognized by its neighborhood, and they may be used in colored and the monochromatic environment. The M arrays can be generated using the method based on the extension of pseudorandom sequence of arrays (PRSA) [7-9] to the bi-dimension case. Vuylsteke and Oosterlinck [10] realized it's hard to generate adequate code words with binary modulation. A novel shape-modulation based on pseudonoise sequences was proposed in their work. A 64*63 grid points with different texture and orientation was generated and used as projecting pattern. Morano et al. [11] proposed a color pattern based on pseudorandom codes. The utilization of colors reduces the size of

window. But it should be made sure the color-coding is feasible. Spoelder et al.[12] evaluated the accuracy and the robustness on color-coded PRBA's. Good results were obtained by using a 65*63 PRBA pattern with window size of 6*2. Petriu et al.[13] also proposed a grid light pattern of 15-by-15 with multi-valued color codification. But the colors used in the proposed pattern were not fixed. This approach generally suited for static sense since it assumed the objects kept stationary during the experiment.

PRSA has a very important window characteristic when a k1×k2 sub-window is moving through in n1×n2 windows（k1<=n1 and k2<=n2）.The mall sub-windows can be recognized uniquely. We bespread a 1024×768 projector plate with code points which occupy 11×11 pixels and spaced by 2 pixel. There will be 79×59 code points on the plate and 4661 code words are produced for global unique codification. And, only are 10 code bits and a minimum sub-window size of 2×2 required to generate such a large number of code words while utilizing monochrome illumination. In order to make best use of symbol's horns and intersections, we choose 10 special symbols. The symbols chosen to be the elements of M array have three characteristics. First, the symbols' size is 11×11, which satisfies the measuring accuracy. Second, the symbols can not be affected by translating, revolving and scaling, so have the high measuring accuracy. Third, the turning points and the intersections of each symbol have provided as far as possible many characteristic point to support to obtain the restructuring data. Figure 9 shows partial image we grabbed by a digital camera based on COMS structure with resolution of 2048×1536 while we projected sub-patterns onto a stair with a projector with resolution of 1024×768.

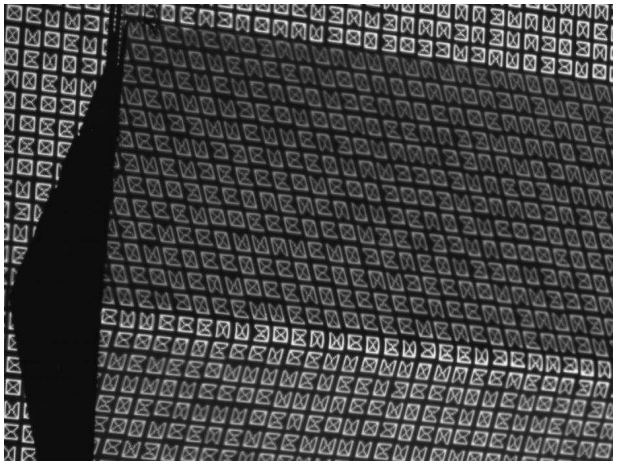

Figure 9. Partial grabbed image

B. Key Points Identification

Horns and intersections of symbols are settled in sub-pattern acting as key points and we realized that these points, such as point 1, 2, 3, 4 and so on shown in Figure 10, have large angle variations.

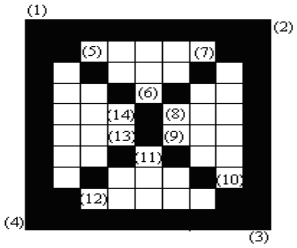

Figure 10. Key points definition

Because there are only several kinds of angle variation, such as 0, 45, 90, 135, 180, 225, 270 and 315 degrees, we take place of evaluating angle variation by its direct conjunct neighbors. We defined the angle variation at one point, point p in Figure 11 for an example, as follow.

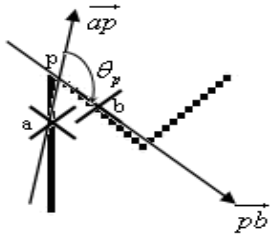

Figure 11. Angle variation

Giving an integer r, and assume *Ip* is the index of point p in contour sequence. Two points a and b can by created at coordinates of equation (10) respectively.

$$x_a = \frac{1}{r}\sum_{i=Ip-r}^{Ip-1} x_i; \qquad y_a = \frac{1}{r}\sum_{i=Ip-r}^{Ip-1} y_i$$
$$x_b = \frac{1}{r}\sum_{i=Ip+1}^{Ip+r} x_i; \qquad y_b = \frac{1}{r}\sum_{i=Ip+1}^{Ip+r} y_i \tag{10}$$

Where x_i and y_i are the coordinates of the point with index of *i* in contour sequence.

Defines vectors $\overrightarrow{ap}$ and $\overrightarrow{pb}$ as

$$\overrightarrow{ap} = complex(x_p, y_p) - complex(x_a, y_a)$$
$$\overrightarrow{pb} = complex(x_b, y_b) - complex(x_p, y_p) \tag{11}$$

Angle variation at point p can be computed as

$$\theta_p = angle(\overrightarrow{pb}) - angle(\overrightarrow{ap}) \tag{12}$$

So, if we always arrange contour sequence at one direction, say clockwise, the angle variations at key points (*KP* for short)1, 2, 3, 4, 5, 7, 10 and 12 will have positive peak values, while the angle variations at points 6, 8, 9, 11, 13 and 14 get negative peak values as shown in Figure 12 and Figure 13.

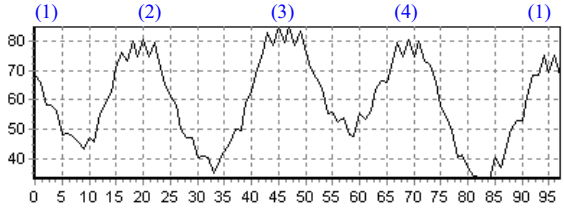

(a)Symbol's outer contour sequence

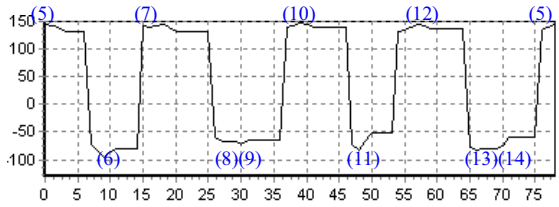

(b)Symbol's inner contour sequence

Figure 12. Angle variation under given integer(r=17)

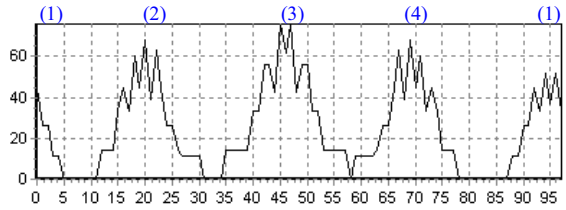

(a)Symbol's outer contour sequence

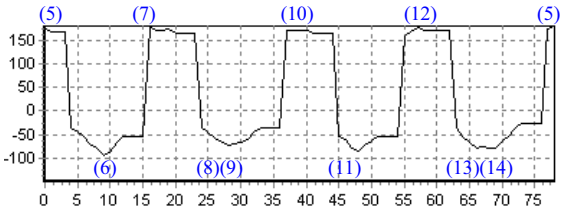

(b)Symbol's inner contour sequence

Figure 13. Angle variation under given integer(r=10)

Figure 12 and Figure 13 show angle variations under different given integer r. X-axis is point index in contour sequence. Y-axis is the angle variation of each point. r equals 17 and 10 respectively in Figure 12 and Figure 13.

Angle variations related closely with the given integer r. A small value of r is capable of view detail information of the chain and a large value of r is helpful to perceive general shape of the chain. We can find in Figure 12 and Figure 13, there would be one negative peak between two successive positive peaks. At the key point, angle variation is larger than other point's. These key spots have the high locating accuracy, which may be seen as the measuring point.

C. 5.3 Symbol Identification and Code Mapping

Different symbols has different angle variation, and there are remarkable difference of the position of positive and negative peaks between different random two symbols At the same time, the sum of positive and negative peaks has difference among these 10 symbols. Because of above features, we may identify robustly 10 kinds of symbols.

We greatly shrunk unknown region in a symbol by the identification of key points. Subsequently, we map unidentified symbols, one by one, to positions in the standard pattern model. We make use of the sub-window global unique characteristic of PRSA to identify symbols and key points 1 to 14 act as reference points through mapping process. Two nearest reference points are chosen to implement mapping action in order to minimize the error. After all code symbols are identified, the code symbols of the sub-pattern can be figured out. Experiment result is shown in Figure 14.

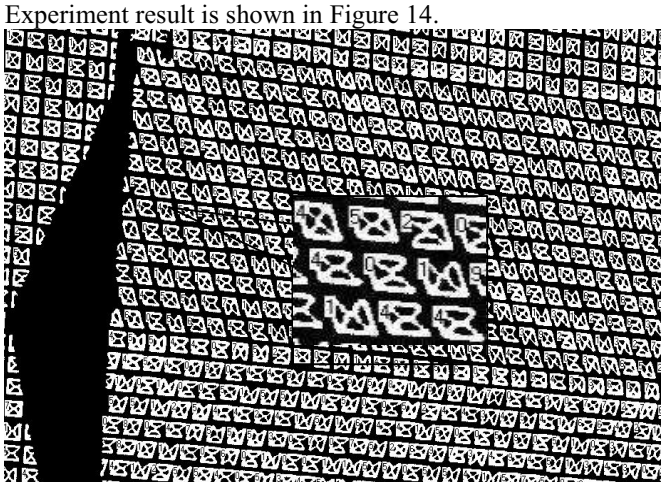

Figure 14. Experimental decoding results on partial image

The program can only cope with integrated sub-patterns at current stage. Figure 14 displays the experimental result while applying above recognition algorithm on partial image of stair. The result shows the algorithm works correctly for integrated sub-patterns.

D. Three Dimensional Reconstruction

Using establishment model, the designed pattern is projected to the object in scene. The CCD grabs scene image. The process of identification of sub-pattern means the establishment of relation between distorted sub-pattern and normal sub-pattern. Using this information, based on the structured light sensing principle [15-16], we can reconstruct 3D outline of objects.

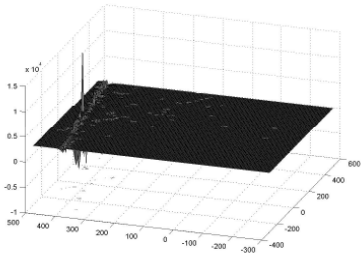

(a) Reconstruction plane

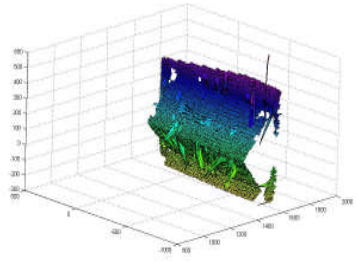

(b) Reconstruction ladder

Figure 15. Reconstruction results

Figure 15(a) and (b) are the reconstruction results of two objects. There are some cavities and burrs. The reasons are: First, because of scene depth influence, partial pattern symbols are broken and incomplete, so decoding algorithms can't recognize them. Second, after symbol image pro-processing, as a result of noise disturbance, partial symbols' contour is broken, which disturbs symbol recognition. Third, there are lost judgment and misjudgment symbols in the course of recognition

We defined two formulas to calculate the recognition rate of symbols and the erroneous judgment rate of sub-window as follow.

$$R\_rate = \frac{S\_sum - ES\_sum}{S\_sum} * 100\% \qquad (13)$$

Where R_rate is the recognition rate of symbols, S_sum and ES_sum are the sum of symbols and the sum of erroneous or omissive judgment symbols respectively.

$$E\_rate = \frac{EW\_sum}{W\_sum} * 100\% \qquad (14)$$

Where E_rate is the erroneous judgment rate, EW_sum and W_sum are the sum of erroneous or omissive judgment sub-windows and the sum of sub-windows respectively.

Using equations (13) and (14), we have calculated the recognition rate and sub-window erroneous judgment rate of a plane and a ladder shown in Table 1.

TABLE 1. THE R_rate AND E_rate OF OBJECTS

Objects	R_rate	E_rate
Plane	99.51%	1.61%
Ladder	98.13%	6.34%

Some valuable conclusions can be obtained from Table 1. The character recognition rate is above 95%, the sub-window erroneous judgment rate is below 7%, which can achieve the basic recognition requirement. Future works will focus on the integration of broken patterns caused by discontinuous surface. With the changing of scene depth, the image of a certain pattern will shift along a certain path. So fractals of the pattern are unlikely to appear in the image unrestrictedly. And with the help of horns in the pattern, which can be used as indicators of fractals, fractals might be scrabbled up and then be submitted to decoding process discussed above.

V. CONCLUSIONS

Recently, the structured light technology is becoming research hot spot in 3D detecting technologies. Structured light technique is a deformation of stereovision, which projects a coded pattern light. It overcomes the question of pixel matching, and its detection is simple, rapid and high efficient. It is an ideal approach of 3D sensing. Structured light detecting technique has extensive requirement and applicative potential in the fields of robot navigation, reversion engineering, object recognition, industrial automation, object tracking, etc.. This paper proposes a simple mathematical model, and simulates using computer. The optimal system parameters are obtained in the experiments, which will support for the structured light technology further application. The 3D reconstruction experiment results show the partial superiority of structured light. So structured light technique research is both of theoretical and applicative value.

REFERENCES

[1] Dalit Caspi, Nahum Kiryati, Joseph Shamir, "Range Imaging with Adaptive Color Structured Light", IEEE Transactions on Pattern Analysis and Machine Intelligence, Vol. 20 , NO. 5(May 1998), pp. 470-480.

[2] Jordi Pagès, Joaquim. Salvi, Carles Matabosch, "Implementation of a Robust Coded Structured Light Technique for Dynamic 3D Measurements", IEEE International Conference on Image Processing, ICIP 2003, vol. 1, Barcelona, Spain(Sep. 2003), pp. 1073-1076.

[3] Jordi Pagès, Assisted Visual Serving by Means of Structured Light. European thesis for the University of Girona and French thesis for the University of Rennes I. Viva: November the 25th, 2005.

[4] Zhong-hai HE, Bao-guang WANG, "Model and Imaging Formula of the Line Structured Light Sensor", Optics and Precise Engineering, Vol. 9, No. 3, 2001, pp. 269-272.

[5] Guo-zhi TAO, Wen LIU, Sheng-hua YE, "The Mathematical Model and Measurement Method of Single Line Structured Light Transducer", Journal of Astronautic Metrology and Measurement, Vol. 19, No. 6, 1999, pp. 51-54.

[6] Guang-jun ZHANG, Jun-ji HE, "Mathematic Model of Inner Surface 3D Vision Inspection Based on Circle Structured Light", Chinese Journal of Scientific Instrument, Vol. 25, No. 4, 2004, pp. 481-484.

[7] Ali A., Halijak C A. "The pseudorandom sequence of arrays", System Theory, 1989. Proceedings., Twenty-First Southeastern Symposium on. 1989,pp. 138-140.

[8] Morita H, Yajima K and Sakata S. "Reconstruction of surfaces of 3-d objects by m-array pattern projection method". Computer Vision, 1988. Second International Conference on, 1988,pp. 468-473.

[9] Kiyasu S, Hoshino H, Yano K, et al. "Measurement of the 3-d shape of specular polyhedrons using an m-array coded light source". Instrumentation and Measurement, IEEE Transactions on,Vol. 44, No. 3, 1995, pp. 775-778.

[10] Vuylsteke, P. A. Oosterlinck, "Range image acquisition with a single binary-encoded light pattern". Pattern Analysis and Machine Intelligence, IEEE Transactions on. Vol.12, No.2 1990, pp.148–164.

[11] Morano, R. Ozturk C., Conn R., Dubin S., Zietz S., Nissano J, "Structured light using pseudorandom codes. Pattern", Analysis and Machine Intelligence, IEEE Transactions on. Vol.20, No. 3, 1998, pp. 322–327.

[12] Spoelder J., Vos F., Petriu E., Croen F., "A study of the robustness of pseudorandom binary-array-based surface characterization", Instrumentation and Measurement, IEEE Transactions on. Vol.47, No.4, 1998, pp. 833–838.

[13] Petriu E. M., Sakr Z., H. J.W. Spoelder, "A. Moica: Object recognition using pseudo-random color encoded structured light", Instrumentation and Measurement Technology Conference, 2000. IMTC 2000. Proceedings of the 17th IEEE. 2000, pp. 1237–1241.

[14] Joaquim Salvi, Jordi Pagès, Joan Batlle. "Pattern Codification Strategies in Structured Light Systems", Pattern Recognition, The Journal of the Pattern Recognition Society, Oct. 2, 2003, pp. 1-23.

[15] Jordi Pagès, Joaquim Salvi, Josep Forest, "A New Optimised De Bruijn Coding Strategy for Structured Light

Patterns". 17th International Conference on Pattern Recognition, (ICPR'04)-Volume 4, 2004, pp. 284-287.

[16] Qing-cang Yu, Xiao-jun Jia, Jian Tao, Yun Zhao, "An Encoded Mini-Grid Structured Light Pattern for Dynamic Scenes". Lecture Notes in Computer Science, v3644. Part I, pp. 126-135.

Xiaojun Jia received his B.E degree from University of Electronic Science and Technology of China in 1999 and M.S degree from Zhejiang Sci-Tech University in 2007. His research focus is computer vision, digital image processing, detecting online and computer education. He has published 10 papers in both technical and educational fields.

Guangxue Yue received her M.S degree from Hunan University, China . Currently, he is working towards the Ph.D. degree in College of computer & communication, Hunan University. His research focus is networking and distributed computing, embedded computation, detecting online and computer education.

Fang Mei received her B.E degree from Zhejiang Sci-Tech University in 2005, and M.S degree from Zhejiang Sci-Tech University in 2008. Her research focus is computer vision, digital image processing, detecting online and computer education.